MODELING OF A DRY COOLING UNIT OPERATED WITH SUPERCRITICAL CO_2 IN 25 MW NDDCT

[1]M. MONJURUL EHSAN, [2]XURONG WANG, [3]ZHIQIANG GUAN, [4]A.Y. KLIMENKO

[1,3,4]School of Mechanical and Mining Engineering, The University of Queensland, Brisbane, QLD 4072, Australia
[2]School of Energy and Power Engineering, Xi'an Jiaotong University, Xi'anShanxi 710049, People's Republic of China
E-mail: [1]m.ehsan@uqconnect.edu.au, [2]wang.xu.rong.1@stu.xjtu.edu.cn, [3]guan@uq.edu.au, [4]a.klimenko@uq.edu.au

Abstract - Dry cooling towers are mostly employed in thermal power plants due to scarcity of water, utilized energy consumption and reduced maintenance cost associated with the mechanical fans. Different types and shapes of natural draft dry cooling towers (NDDCT) are used in many thermal and power plant industries whose main purpose is to generate air flow through the finned tube heat exchanger bundles by the influence of buoyancy due to density difference between fresh ambient air and warm exit air. In the present article, we develop an one dimensional MATLAB code to design a 25 MW capacity NDDCT with detailed specification of finned tube heat exchanger bundles operated with supercritical CO2 (sCO2). The tower height, tower inlet and outlet diameters, number of heat exchanger bundles and total air side and tube side areas are evaluated after accomplishing the design of the tower according to specified. The profiles for temperature, heat rejection and convective heat transfer coefficient for both air side and sCO2 side and the characteristics of pressure drop are comprehensively investigated to evaluate the performance the an air cooled heat exchanger unit.

Keywords - Cooling tower, supercritical CO2, heat transfer, heat exchanger.

I. INTRODUCTION

The superior thermo-physical properties and minimal environmental hazards such as low global warming and ozone depletion empower supercritical CO_2 (sCO_2) as one of the promising refrigerant substitutes in refrigeration and air conditioning technology. In last few decades, researchers have been emphasized to explore the application of sCO_2 as a working fluid in nuclear and thermal power plant industries. The supercritical CO_2 power cycles are anticipated as one of the next generation power cycles due to lower operation cost and simplified plant design. For smooth and efficient operation, all thermal power plant need reliable cooling method to cool the turbine exhaust. The thermal efficiency of any power plant is maximized with maximum heat source temperature and lowest possible heat sink temperature. Therefore, cooling tower is an essential element of a cooling system for smooth and efficient operation of the power plant.

The implementation of sCO_2 in traditional closed loop Brayton cycle can considerably reduce the compressor work, plant running cost and improve the overall thermal efficiency. It allows the compression process without intercooling, lesser turbine stages and the use of more compact heat exchangers [1]. The first closed loop regenerative Brayton cycle was proposed by Feher [2], where the compression process was conducted with a pump to handle the high density of sCO_2. Dostal et al. [1] proposed various sCO_2 Brayton cycles and higher efficiency was achieved with recompression Brayton cycle in comparison with helium Brayton cycle. Conboy et al. [3] investigated the influence of turbine and compressor inlet temperatures on the effectiveness of sCO_2 Brayton cycles with dry air cooled heat exchanger unit. Osorio et al. [4] analysed the dynamic characteristics of sCO_2 Brayton cycle for concentrated solar power plant under various seasonal conditions using forced draft dry cooling tower. Singh et al. [5] also performed the influence of solar heat input, mass flow rate, and operating pressure on the net power output of sCO_2 recuperated Brayton cycle coupled with direct dry cooling towers. Padilla et al. [6] employed dry coolers to perform the energy and exergy analysis with four different sCO_2 Brayton cycle configurations. Conradie and Kroger [7] conducted the performance evaluation for both natural draft and mechanical draft cooling towers. Zheng et al. [8] employed solar collector to enhance the thermal effectiveness of a natural draft dry cooling tower. Tanimizu and Hooman [9] performed preliminary numerical and experimental studies with NDDCT, where heat exchanger was arranged in vertical and horizontal configuration.

In the present article, a validated one-dimensional MATLAB code is generated to design a 25 MW NDDCT operated with sCO_2. The present code is able to predict the heat transfer mechanism and flow behaviour for both air side and sCO_2 side of a finned tube heat exchanger. The extreme variation of thermo-physical properties of sCO_2 in the vicinity of critical region is well captured by the present code. The changes of various thermodynamic and transport properties along the tube length and as well as across the tube bundles are scrutinised.

II. SCO_2 BRAYTON CYCLE LAYOUT

Fig. 1 demonstrates a typical closed loop sCO_2 Brayton cycle, where sCO_2 after following the expansion process in turbine is sent to the recuperator to reject some of the heat and preheat the compressor outlet sCO_2 stream before entering in to the cooling tower. Air-cooled heat exchanger unit transfers the heat from the sCO_2 to the fresh air stream, which flows

across the finned tube heat exchanger bundles. Various flow resistances at different sections of a NDDCT are experienced by the air stream and these flow resistances cause significant pressure drop for which the hot air is discharged at a moderate velocity through the outlet of the cooling tower by the influence of draft force. In the present article, concentration has been paid within the NDDCT. For a power plant capacity of 25 MW with 49% thermal efficiency, the required size and specification for the heat exchanger and cooling tower are designed by employing a validated one dimensional MATLAB code. The program is developed to meet the duty requirements with some given input parameters (Ambient air temperature, atmospheric pressure and sCO_2 inlet temperature and pressure).

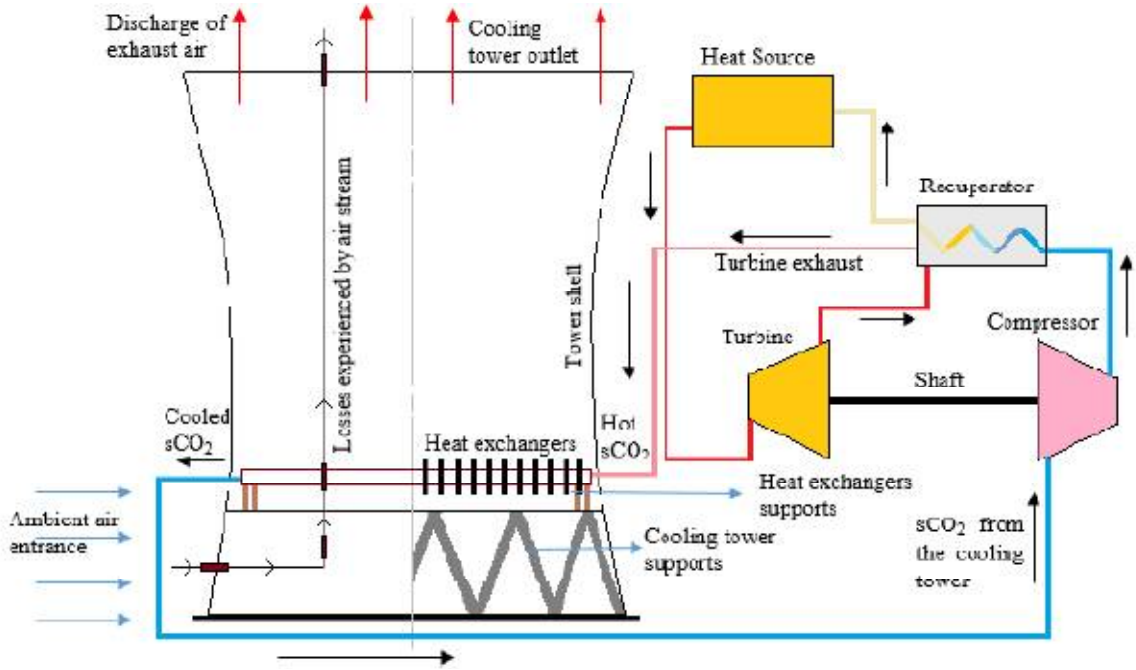


Fig. 1. A typical air cooled heat exchanger unit to cool sCO_2 in a NDDCT.

III. ANALYSIS OF NDDCT

Natural draft dry cooling towers are available in thermal and nuclear power plant industries whose main task is to produce air flow by means of buoyancy effect. The change of pressure causes the air flow through the outlet of the tower. The larger the density difference and elevation of the tower, the higher the buoyant force. The volume flow rate of air through the bundles of heat exchanger is dependent on the temperature difference and the height of tower. The height of the cooling tower can be up to 200 m tall [10]. The pressure differential in the tower is a function of different flow resistances experienced by the inlet air while flowing through different sections of the cooling tower [11]. The energy equation for a NDDCT can be expressed by the following equation.

$$Q_a = M_a C_{pa34}(T_{a4} - T_{a3}) = Q_s = M_s C_s(T_{si} - T_{so})$$

$$Q_{hx} = \frac{UA\,F_T[(T_{si} - T_{a4}) - (T_{so} - T_{a3})]}{\ln\left[\frac{(T_{si} - T_{a4})}{(T_{so} - T_{a3})}\right]}$$

The air stream at the entrance of the cooling tower experiences losses (K_{ts}) due to cooling tower support from section 1 to 2, as shown in Fig. 2. Again, losses are encountered by the air stream known as cooling tower inlet loss (K_{ct}) due to separation of flow, distortion of inlet flow pattern and redirection of air flow. The supports of heat exchangers also exert some losses known as heat exchanger support loss (K_{hes}) from section 2 to section 3. Air stream, while flowing across the finned tube heat exchanger bundles from section 3 to section 4 are encountered with certain losses as: contraction losses (K_{ctc}), expansion losses (K_{cte}) and frictional losses (K_{he}). The flow from section 4 to section 5 is essentially an isentropic flow where the hot air experiences further loss in kinetic energy, known as cooling tower outlet loss coefficient (K_{ct}). By adding all the flow resistances, the total pressure difference between section 1 and 5 is calculated by the following equation, known as the draft equation.

$$p_{a1} - \left[p_{a5} + \frac{\left(\frac{m_a}{A_5}\right)^2}{2\rho_{a5}}\right] = (K_{ts} + K_{ct} + K_{hes} + K_{ctc} + K_{he} + K_{cte})\frac{\left(\frac{m_a}{A_{fr}}\right)^2}{2\rho_{a34}} + p_{a1}\left[1 - \left\{1 - 0.00975\frac{(H_3 + H_4)}{2T_{a1}}\right\}^{3.5}\right] + p_{a4}\left[1 - \left\{1 - 0.00975\left(H_5 - \frac{H_3}{2} - \frac{H_4}{2}\right)T_{a4}\right\}^{3.5}\right]$$

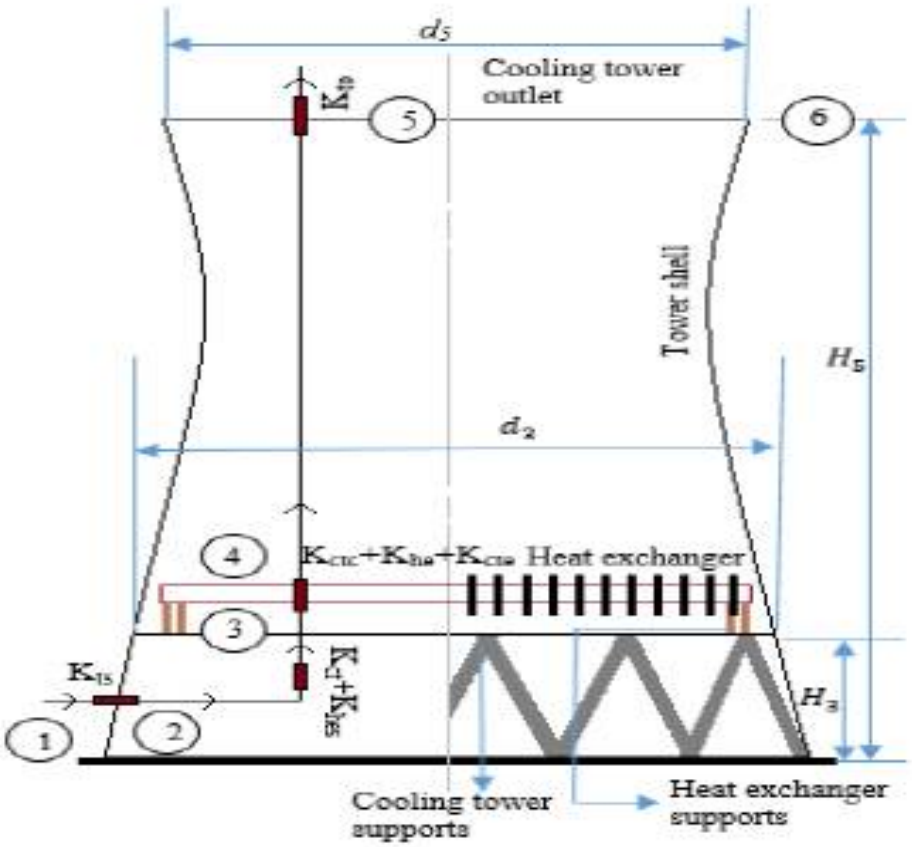


Fig. 2 Various flow resistances experienced by air in NDDCT

Tube side specification			*Fin side specification*		
Parameter	*Value*	*Unit*	*Parameter*	*Value*	*Unit*
Tube material	ASTM A214 mild steel		Fin type	Extruded bimetallic	
Thermal conductivity of the tube, k_t	50	W/mK	Heat exchanger arrangement	horizontal	-
Tube outside diameter, d_o	25	mm	Fin shape	circular	-
Tube inside diameter, d_i	20	mm	Tube arrangement	staggered	-
Relative tube surface roughness, ε/d_i	5.24×10^{-4}		Fin material	ASTM 6063 aluminium	
Number of tube rows, n_r	4	-	Thermal conductivity, k_f	204	W/mK
Effective no. of tubes per row, n_{tr}	47.5	-	Fin diameter, d_f	57	mm
No. of tubes per bundle, n_{tb}	190	-	Fin root diameter, d_r	28	mm
Transversal tube pitch, P_t	58	mm	Fin shape	Tapered	-
Longitudinal tube pitch, P_l	52	mm	Fin tip thickness, t_{ft}	0.25	mm
Length of the finned tube, l_t	6	m	Fin thickness (mean), t_f	0.5	mm
Width of the heat exchanger	2.47	m	Fin root thickness, t_{fr}	0.75	mm
Height of the heat exchanger	0.232	m	Fin pitch, P_f	2.8	mm

Table 1: Specification Heat Exchanger model

Parameter	*Value*	*Unit*
Aspect ratio of cooling tower, H_5/d_3	1.4	-
Tower inlet height, H_3	10	m
Tower Diameter ratio, d_5/d_3	0.7	-
Heat exchanger coverage of tower inlet, A_{frT}/A_3	0.7	-
Number of tower supports: n_{ts}	$d_3/1.38$	-
Length of tower support: *lts*	$H_3 \times 1.15$	m
Drag coefficient of support, C_{Dts}	2	-
Diameter of tower support, d_{ts}	0.5	m

Table 2: Specified parameters for 25 MW NDDCT analysis

IV. ANALYSIS OF AIR COOLED HEAT EXCHANGER UNIT

Air cooled heat exchanger unit transfers the heat of the working fluid to the fresh air stream flowing across the bundles of tubes by means of extended surfaces or fins. The convective heat transfer coefficient of air is considerably lower than the working fluid flowing inside the tubes, hence the surface area of the air side is enhanced by the implementation of different types of fins on the bare tubes in order to accomplish the required cooling. For calculation of overall heat transfer coefficient of a finned tube heat exchanger, following are the assumption made.

a) The base of the fin also conducts heat and there is no internal heat generation by the fin.
b) Heat transfer through fins is one dimensional steady state heat conduction and convection.
c) The thermal conductivity of the fins are constant and fins are perfectly bonded with bare tubes with zero thermal contact resistance.

V. MODEL SET UP AND PREPERATION

In the proposed NDDCT model, a number of air cooled finned tube heat exchangers are employed to exchange heat from the hot sCO_2. Table 1, shows the specification of heat exchanger specification, where the heat exchanger is arranged horizontally and the tubes are arranged in staggered configuration. Each bundle contains 190 tubes and number of required bundles to meet the duty requirement is evaluated from the present code. The heat exchanger is modelled as four tube rows and one pass. The program is developed to model a 25 MW NDDCT with 49% thermal efficiency operating under sCO_2 inlet temperature of 71°C, operating sCO_2 pressure of 7.5 MPa, ambient temperature of 20°C and atmospheric pressure of 99695 N/m^2. The required amount of sCO_2mass flow rate is determined from the plant capacity. The values for various geometric parameters are considered from Kroger [12] one dimensional model of NDDCT are shown in table 2.

In order to evaluate the overall heat transfer coefficient of the heat exchanger, the convective heat transfer for both air side and sCO_2side are required. For this purpose, the air side heat transfer coefficient is evaluated from the most recommended Briggs and Young [13] correlation.

$$\frac{h_a d_r}{k_a} = 0.134 Pr_a^{0.33} Re_a^{0.681} \left[\frac{2(P_f - t_f)}{d_f - d_r}\right]^{0.2} \left(\frac{P_f - t_f}{t_f}\right)^{0.1134}$$

The sCO_2 heat transfer coefficient is evaluated by means of Yoon et al. [14] suitable for cooling of sCO_2 in macro tube geometries.

$$Nu_s = \frac{h_s d_s}{k_s} = a Re_s^{\,b} Pr_s^{\,c} \left(\frac{\rho_{pc}}{\rho_s}\right)^n$$

a=0.14, b=0.69, c=0.66, n=0 when $T_b > T_{pc}$
a=0.013, b=1.0, c=-0.05, n=1.6 when $T_b \leq T_{pc}$

For air side pressure drop calculation, Robinson and Briggs [15] correlation is applied.

$$f_a = 9.465 Re_a^{-0.316} \left(\frac{P_t}{d_o}\right)^{-0.927} \left(\frac{P_t}{P_d}\right)^{0.515}$$

Following friction factor equation proposed by Churchill [16] is used to evaluate the sCO_2 side pressure drop.

$$f_s = 8\{\left(\frac{8}{Re_s}\right)^{12} + [2.457 \ln \left(\frac{1}{\left(\frac{7}{Re_s}\right)^{0.9} + 0.27\frac{\varepsilon}{D}}\right)^{16} + \left(\frac{37530}{Re_s}\right)^{16}]^{-1.5}\}^{\frac{1}{12}}$$

The properties of sCO_2 (specific heat, density, thermal conductivity and viscosity) are measured by linking the MATLAB with the software package REEFPROP 9.0 [17].

VI. MATHEMATICAL MODEL

The extreme variation of thermodynamic properties of sCO_2 in the vicinity of critical point is one of the key challenges associated with the Modeling of NDDCT. In the present code, a nodal approach is adopted to capture the drastic property variation of sCO_2 in the heat exchanger, shown in Fig. 3. In the nodal approach, each row of tubes of the heat exchanger bundles is divided into 30 sections. Therefore, the length of each section is 200 mm. For each section, inlet temperature of sCO_2 and air are known and calculation starts with an initial assumption of outlet temperatures. The energy equation is satisfied for each section and the output parameters are considered as inputs for the next section. The convective heat transfer coefficient and pressure drop for both air side and sCO_2 side are calculated for each small section. After calculation of first row of tubes, the air outlet temperatures and pressures are taken as input for second row of tubes. Similarly for all the remaining row of tubes, the local heat transfer and pressure drop are calculated.

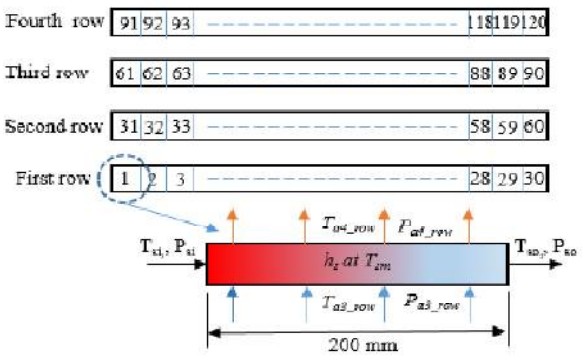


Fig. 3. Nodal approach for heat exchanger model

The total heat rejected by the tower is the sum of heat transfer in all 120 sections. Therefore, if the total heat rejection does not meet the tower requirements, the code modifies the tower height. The required height of cooling tower is evaluated once it satisfies the total heat rejection requirement. All the optimum parameters (tower specification, number of heat exchanger bundles and mean outlet temperatures) after calculation are shown in table 3.

Parameter	Value	Unit
Outlet height of tower, H_5	50.622	m
Outlet tower diameter, d_5	25.31	m
Inlet tower diameter, d_3	36.16	m
Number of heat exchanger bundles, n_b	49	-
Number of tower supports: n_{ts}	27	-
Length of tower support: *lts*	11.5	m
Total air side area	85,797	m^2
Total tube side area	3,510	m^2
sCO_2 mean outlet temperature, T_{so}	40.36	^oC
Air mean outlet temperature, T_{o4}	43.4	^oC
Air mass flow rate, M_a	1107	Kg/sec

Table 3: Optimum parameters for a 25 MW NDDCT

RESULTS

A. Study of temperature profiles

Fig. 4 demonstrates the temperature profile of sCO_2 along the length of heat exchanger tube bundles for each row, for an ambient air temperature of 20°C and inlet sCO_2 temperature of 71°C flowing under an operating pressure of 7.5 MPa. For the first tube row, sharp decrease of sCO_2 temperature is observed, whereas for second, third and last tube rows, slope of the temperature profile is less steeper since the air temperature gradually rises across each tube row.

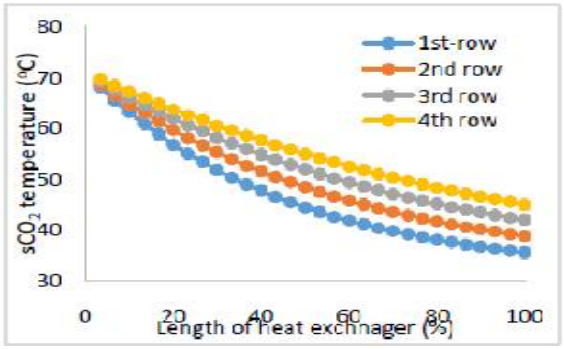


Fig. 4. sCO_2 temperatures along the length of heat exchanger bundles.

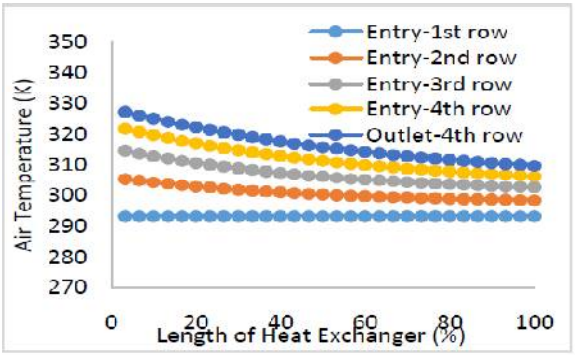


Fig. 5. Air outlet temperatures profile.

Fig. 5 shows the air temperature profile across each tube row and along the length of heat exchanger tube bundles for the same operating conditions. As the heat is transferred by hot sCO_2, air temperature rises monotonously across each tube rows. The ambient air temperature is same for the first tube row, which is reflected by a straight horizontal line. However, after air flowing across the first tube row, air temperature decreases along the length of pipes. Initially at the start of the tubes, the air temperature is higher than temperature at the end of pipes since the inlet temperature of sCO_2 is high and same for each tube row.

B. Study of convective heat transfer coefficient

The variation of forced convective heat transfer coefficient of sCO_2 along the length of heat exchanger bundles and across each tube row is shown in Fig. 6, for an ambient air temperature of 20°C, sCO_2 inlet temperature of 71°C and operating pressure 7.5 MPa. As the bulk temperature of sCO_2 decreases, convective heat transfer coefficient increases along the length of pipe. For the first tube row, sCO_2 heat transfer coefficient is increased remarkably due to higher temperature difference between inlet sCO_2 and ambient air and lower bulk temperatures. For the second, third and last row, the slope is less steeper as the air temperature rises across the tube row and causes less improvement of sCO_2 heat transfer coefficient along the length of the pipe. Average air side heat transfer coefficient across each tube row, is shown in Fig. 7. An increase of mean air outlet temperature across each tube row causes very small increment of the air side heat transfer coefficient due to changes of air thermodynamic properties.

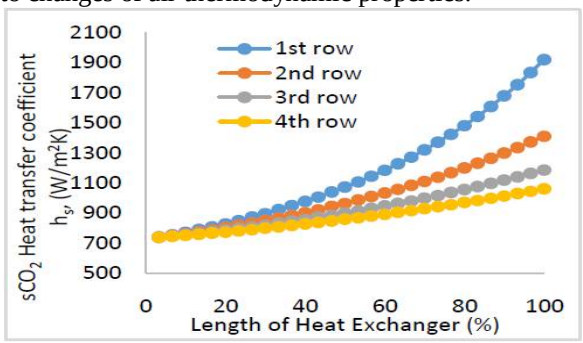


Fig. 6. sCO_2 heat transfer coefficient along the length of heat exchanger bundles.

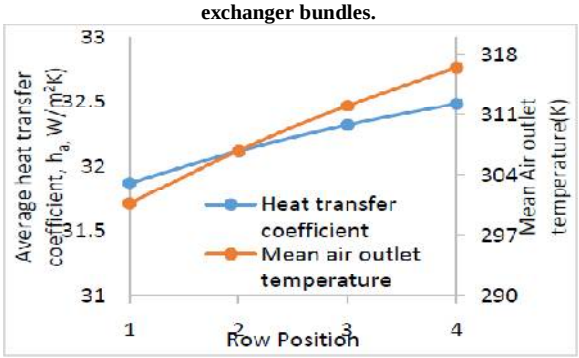


Fig. 7. Air side heat transfer coefficient across the heat exchanger bundles.

C. Study of pressure drop characteristics

Fig. 8 reveals the pressure drop variation along the length of the pipe and across the tube row. Variation of pressure drop at the inlet of tube is more dominant due to higher Reynolds number. Along the tube length, bulk temperature of sCO_2 gradually decreases which causes the flow Reynolds number to be decreasesd gradually due to increased density and viscosity at lower bulk temperature. Therefore, pressure drop decreases along the tube length and the total pressure drop at the end of each row of tubes increases essentially due to increase of ambient air temperature. At any position along the tube length, as the row position is increased, bulk temperature of sCO_2 increases. Increased bulk temperature provides higher values of Reynolds number due to decreased viscosity. The total pressure drop at the end of heat exchanger tube bundles for each tube row are 3.13 kPa, 3.31 kPa, 3.45 kPa and 3.56 kPa respectively.

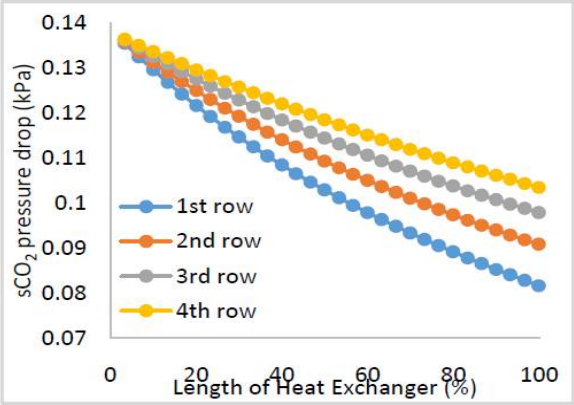


Fig. 8. sCO_2 pressure drop variation along the length of heat exchanger bundles.

The variation of air side pressure drop across the heat exchanger tube bundles is shown in Fig. 9. Air side pressure drop more or less remains constant along the tube length although at the inlet of tubes, the pressure drop is slightly higher due to higher temperature difference between sCO_2 and air. Air side Reynolds number and Prandtl number show minor decrease across each tube row but the thermal conductivity of air increases with temperature, which causes slight increase of pressure drop. The total air side pressure drop is 113.16 Pa.

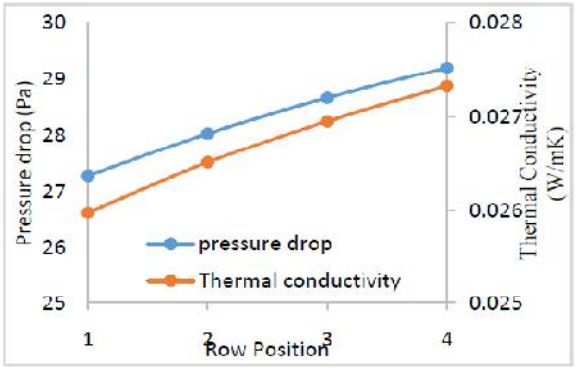


Fig. 9. Air side pressure drop across the heat exchanger bundles.

D. Heat rejection profiles

Fig. 10 demonstrates the sCO_2 heat rejection variation along the length of the pipe and across the tube row under an operating condition: sCO_2 inlet temperature 71°C, inlet pressure 7.5 MPa, ambient air pressure 99695 Pa and ambient air temperature 20°C. Heat rejection decreases along the length of the pipe due to the gradual decrement of temperature difference between air and sCO_2. Total heat rejected by sCO_2 for each tube rows are 8.38 MW, 6.9 MW, 5.81 MW and 4.96 MW respectively. Maximum heat rejection is obtained from the first tube rows due to maximum temperature difference between ambient air and sCO_2.

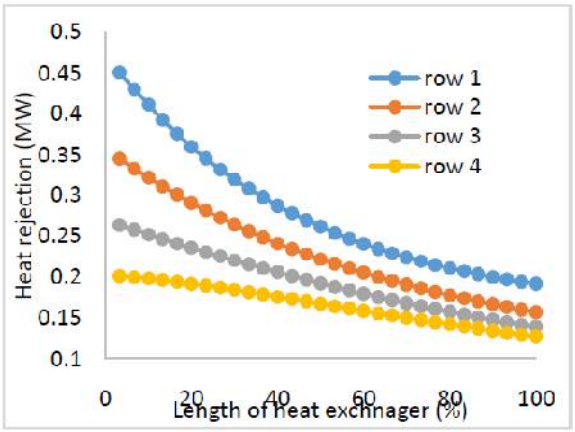


Fig. 10. Heat rejection variation along the length of heat exchanger bundles.

CONCLUSION

Due to scarcity of water and other environmental issues associated with water (water loss due to evaporation, corrosion, dissolved solids, scale deposition and unwanted and unexpected accumulation of sediments), dry cooling systems provide an alternative solution as a heat rejection method in geothermal power plants. The present MATLAB code provides the design specification of a 25 MW NDDCT with detailed geometric parameters of a finned tube heat exchanger unit. Detailed temperature profiles and heat transfer profiles are reported with an effect of different operating parameters. From first row of tubes, highest amount of heat 8.38 MW is rejected, since sCO_2 bulk temperature is much lower and close to the pseudocritical temperature in comparison with the remaining rows of tubes. The highest heat transfer coefficient of sCO_2 is obtained at the end of first row of tubes. Air temperature and pressure monotonously increase across the tube rows of heat exchanger. Finally. the physical phenomenon behind the heat transfer mechanism and pressure drop characteristics are also described.

ACKNOWLEDGEMENT

This research was conducted as a part of the Australia Solar Thermal Research Initiative (ASTRI), a project supported by Australia government through the

Australia Renewable Energy Agency (ARENA). The first author, M. Monjurul Ehsan would also like to acknowledge University of Queensland (UQ) for providing Research Training Program (RTP) and Australian Postgraduate Award (APA) scholarships.

REFERENCES

[1] V. Dostal, M. J. Driscoll, P. Hejzlar, and N. E. Todreas, "A supercritical CO2 gas turbine power cycle for next-generation nuclear reactors," Proc. of ICONE, vol. 10, p. 2002, 2002.

[2] E. G. Feher, "The supercritical thermodynamic power cycle," Energy conversion, vol. 8, no. 2, pp. 85-90, 1968.

[3] T. Conboy, S. Wright, J. Pasch, D. Fleming, G. Rochau, and R. Fuller, "Performance characteristics of an operating supercritical CO2 Brayton cycle," Journal of Engineering for Gas Turbines and Power, vol. 134, no. 11, p. 111703, 2012.

[4] J. D. Osorio, R. Hovsapian, and J. C. Ordonez, "Dynamic analysis of concentrated solar Supercritical CO 2-based power generation closed-loop cycle," Applied Thermal Engineering, vol. 93, pp. 920-934, 2016.

[5] R. Singh, S. A. Miller, A. S. Rowlands, and P. A. Jacobs, "Dynamic characteristics of a direct-heated supercritical carbon-dioxide Brayton cycle in a solar thermal power plant," Energy, vol. 50, pp. 194-204, 2013.

[6] R. V. Padilla, Y. C. S. Too, R. Benito, and W. Stein, "Exergetic analysis of supercritical CO 2 Brayton cycles integrated with solar central receivers," Applied Energy, vol. 148, pp. 348-365, 2015.

[7] Conradie and D. Kröger, "Performance evaluation of dry-cooling systems for power plant applications," Applied Thermal Engineering, vol. 16, no. 3, pp. 219-232, 1996.

[8] Z. Zou, Z. Guan, H. Gurgenci, and Y. Lu, "Solar enhanced natural draft dry cooling tower for geothermal power applications," Solar Energy, vol. 86, no. 9, pp. 2686-2694, 2012.

[9] K. Tanimizu and K. Hooman, "Natural draft dry cooling tower modelling," Heat and Mass Transfer, vol. 49, no. 2, pp. 155-161, 2013.

[10] D. Busch, R. Harte, W. B. Krätzig, and U. Montag, "New natural draft cooling tower of 200 m of height," Engineering Structures, vol. 24, no. 12, pp. 1509-1521, 2002.

[11] F. Moore, Effects of Aerodynamic Losses on the Performance of Large Dry Cooling Towers. 1978.

[12] D. G. Kröger, Air-cooled heat exchangers and cooling towers. PennWell Books, 2004.

[13] D. E. Briggs and E. H. Young, "Convection heat transfer and pressure drop of air flowing across triangular pitch banks of finned tubes," in Chem. Eng. Prog. Symp. Ser, 1963, vol. 59, no. 41, pp. 1-10.

[14] S. H. Yoon, J. H. Kim, Y. W. Hwang, M. S. Kim, K. Min, and Y. Kim, "Heat transfer and pressure drop characteristics during the in-tube cooling process of carbon dioxide in the supercritical region," International Journal of Refrigeration, vol. 26, no. 8, pp. 857-864, 2003.

[15] K. K. Robinson and D. E. Briggs, "Pressure drop of air flowing across triangular pitch banks of finned tubes," in Chem. Eng. Prog. Symp. Ser, 1966, vol. 62, no. 64, pp. 177-184.

[16] S. W. Churchill, "Friction-factor equation spans all fluid-flow regimes," Chemical engineering, vol. 84, no. 24, pp. 91-92, 1977.

[17] E. W. Lemmon, M. L. Huber, and M. O. McLinden, "NIST reference fluid thermodynamic and transport properties–REFPROP," ed: version, 2002.

★★★